Warm Rainy Clouds and Droplet Size Distribution

NAZARIO D. RAMIREZ-BELTRAN[1], ROBERT J. KULIGOWSKI[2], MELVIN J. CARDONA[3] and SANDRA CRUZ-POL[3].

[1]Department of Industrial Engineering, University of Puerto Rico, P.O. Box 9030, Mayagüez, PR 00681, U.S.A, nazario@ece.uprm.edu

[2]NOAA/NESDIS Center for Satellite Applications and Research (STAR), Camp Springs, MD 20746, U.S.A. Bob.Kuligowski@noaa.gov

[3]Department of Computer and Electrical Engineering, University of Puerto Rico, P.O. Box 9040, Mayagüez, PR 00681, U.S.A, cardonam@gmail.com, SandraCruzPol@ieee.org,

Abstract – This paper presents the analysis of cloud droplet size distribution (DSD) and the use of a proxy variable for the parameters of the DSD to explore the possibility of detecting warm rainy clouds. Cloud DSD plays a paramount role in the parameterization of cloud microphysics in climate models. The droplet size distribution also plays a crucial role in determining the radiative properties of clouds and is usually obtained using satellite retrieval algorithms. This paper presents an analysis of the modified Gamma model which is used to represent the cloud DSD. The analysis of the DSD is conducted through the derivation of the distribution moments and their physical interpretation. The analysis includes the discussion of the mean, variance, effective radius, and effective variance of the DSD. Usually the effective radius is extracted from radiance measurements. However, since the modified Gamma distribution has two parameters it requires estimates of both the effective radius and effective variance to properly estimate cloud microphysics from radiance information.

Key-words - Warm rainy clouds, droplet size distribution, modified Gamma distribution, effective radius, effective variance.

1. Introduction

Effective radius is one of the key parameters used in calculation of the radiative properties of liquid water clouds. Slingo [1] studied the sensitivity of the global radiation budget to effective radius and found that the warming effect of doubling CO_2 concentrations could be offset by reducing the effective radius by approximately 2 μm. Kiehl and Briegleb [2] found that a number of known biases in the Community Climate Model 1 (CCM1) were reduced and important changes in cloud radiative forcing, precipitation, and surface temperature occurred if different values of effective radius were assigned to warm maritime and continental clouds. A high sensitivity to the method of parameterizing effective radius was also found by the French Community Climate model [3]. Recently, Comarazamy et al. [4] used the Regional Atmospheric Modeling System (RAMS) with the

new cloud microphysics module described by Saleeby and Cotton [5]. The new RAMS includes two major features: 1) the activation of cloud condensation nuclei (CCN) and giant CCN, and 2) the inclusion of the Gamma distribution to model the droplet size distribution (DSD). Comarazamy et al. (2005) showed that this cloud microphysics module significantly improved RAMS rainfall forecasts over the western part of Puerto Rico.

Hansen [6] established a link between the DSD and single scattering albedo at 3.4 μm. He pointed out that the DSD is sufficient to identify cloud type and different changes in the cloud state by means of the polarization of reflective sunlight. He also showed that the single scattering depends on the DSD and on the real and imaginary parts of the refractive index of the spheres. It is known that the polarization for single scattering is sensitive to the particle size at most scattering angles. This is because the absorption coefficient of water at 3.4 μm is such that the transmission of rays which are refracted into the sphere varies significantly with particle size.

Lindsey and Grasso [7] discussed the development of ice cloud effective radius retrieval for ice clouds using three bands of the Geostationary Operational Environmental Satellite (GOES) imager: visible (0.65 μm), near infrared (3.9 μm), and thermal channel (10.7 μm). They developed an algorithm to compute ice cloud effective radius retrieval for thick ice clouds. This algorithm offers the possibility of monitoring the evolution of thunderstorm-cloud top properties.

Since the DSD plays a very important role in climate models and in extracting cloud microphysics properties from radiative retrieval algorithms, a statistical analysis of this distribution is discussed in this paper. The second section of this paper presents a detailed description of the modified Gamma distribution which is one of the preferred models for representing the DSD. The third section presents Monte Carlo simulation results of the DSD, and a description of the statistical methods for estimating the parameters of the Gamma distribution. The fourth section presents the evolution of effective radius for some pixels from a thunderstorm-top cloud. The fifth section presents the use of a proxy variable for the parameters of DSD to detect the warm rainy clouds. The sixth section presents some conclusions and a summary of the paper, and the Appendix presents some mathematical developments.

2. Cloud droplet size distribution

The reflection function at a water (or ice) absorbing channel in the near-infrared is primarily a function of cloud particle size [8]. The reflection function represents the albedo of the medium that would be obtained from a directional reflectance measurement. .

Cloud DSD is usually represented by different mathematical models such as Lognormal, Gamma and/or modified Gamma distribution ([8]; [6]; [9] [10]). However, the modified Gamma distribution is preferred over the Lognormal since the parameters of the modified Gamma distribution are equal to physical parameters which can characterize the scattering of the size distribution [6]. The modified Gamma distribution can be expressed as follows:

$$n(r) = Lr^{\left(\frac{1}{b}-3\right)}e^{-r/ab}, \qquad (1)$$

$$r > 0, \quad a > 0, \quad and \quad 0 < b < 1/2$$

where r is the radius of a water droplet, assuming that the water droplets have a spherical shape; a and b are the parameters of the probability distribution function, and L is a scaling constant that is necessary for a probability distribution function. That is, in order to be a probability density function the following integral must be satisfied: $\int_0^\infty n(r)dr = 1$. and so after solving the previous integral it can be shown that $L = \frac{(ab)^{(2-1/b)}}{\Gamma\left(\frac{1-2b}{b}\right)}$, where $\Gamma(m)$ is the Gamma function defined as:

$$\Gamma(m) = \int_0^\infty x^{m-1}\, e^{-x} dx. \qquad (2)$$

The parameter a is called the effective radius and b is the effective variance. These parameters have been selected in this way to have a physical interpretation. Thus, to properly interpret the meaning of these parameters, the moment of the k^{th} order of the droplet size distribution will be computed as follows:

$$E(r^k) = \int_0^\infty r^k n(r) dr$$

$$= L(ab)^{\left(k-2+\frac{1}{b}\right)} \Gamma\left(k-2+\frac{1}{b}\right) \qquad (3)$$

Derivation of the formulas is given in appendix. The expected (average) value of a droplet radius is:

$$E(r) = a(1-2b) \qquad (4)$$

The variance of the water droplet radius, which is the expected deviation of each radius from the typical radius, is:

$$V(r) = a^2 b(1-2b) \qquad (5)$$

It should be noted that the effective radius is different from the expected radius and different from the variance of the radius. The effective radius (r_e) is defined as the ratio of the third and second moment of the DSD:

$$r_e = \frac{E(r^3)}{E(r^2)} = a \qquad (6)$$

It should be noted that the effective radius has a geometrical interpretation: it is approximately equal to the ratio of expected volume of a sphere with radius r to the expected area of a circle of radius r. This, ratio can be computed as follows:

$$\frac{E(V)}{E(A)} = \frac{E\left(\frac{4}{3}\pi r^3\right)}{E(\pi r^2)} = \frac{4}{3}\frac{E(r^3)}{E(r^2)} = \frac{4}{3} r_e \qquad (7)$$

where $E(V)$ is the expected volume and $E(A)$ is the expected area of water droplets that come from a population with a modified Gamma distribution (eq. 1). The r is a random variable associated to the radius of each water droplet. Thus, the effective radius can also be defined as follows:

$$r_e = \frac{3}{4}\frac{E(V)}{E(A)} = \frac{3}{4}\frac{\int_0^\infty \frac{4}{3}\pi r^3 n(r) dr}{\int_0^\infty \pi r^2 n(r) dr} \qquad (8)$$

Figure 1 shows the schematic representation of the effective radius. Suppose there is a random sample of droplet size from a modified Gamma population. Suppose further that the average of the volume and the average of the projected area of a sphere are computed. Thus, the effective radius will be the ratio of the two averages as shown in the Fig. 1.

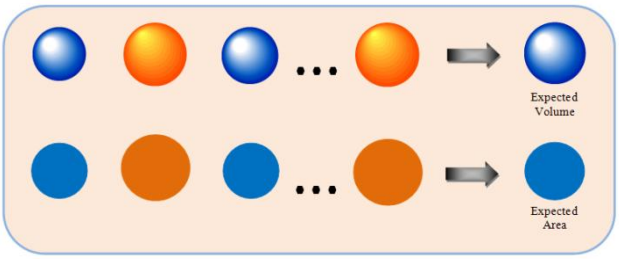

Fig. 1. Graphical representation of effective radius

The effective variance can be defined as the ratio of the expected deviation of the radius from effective radius to the second moment of the DSD, and can be expressed as follows:

$$V_e = \frac{\int_0^\infty (r-a)^2 r^2 n(r) dr}{a^2 \int_0^\infty r^2 n(r) dr} = b \qquad (9)$$

It should be mentioned that the extra term r^2 in the numerator and a^2 in the denominator of equation (9) are required to make the V_e dimensionless and a relative measurement of the droplet size variability.

It is also important to mention that the mean and variance of the DSD are functions of the parameters a and b. However, the effective radius and effective variance are directly related to the single parameters a and b, respectively. Therefore, since the mean (eq. 4) and the variance (eq. 5) of the DSD depend on both a and b parameters (if V_e is fixed and only r_e changes or vice versa), this implies that the scale and

the shape of the probability distribution are modified. This observation has a significant impact on satellite retrieval algorithm of cloud properties [9]. Figure 2 shows the behavior of the modified Gamma distribution when effective variance is fixed at 0.13 nd the effective radius ranges from 3 to 32 μm. Figure 3 shows the behavior of the DSD when the effective radius is fixed at 12 μm, while the effective variance varies from 0.05 to 0.3.

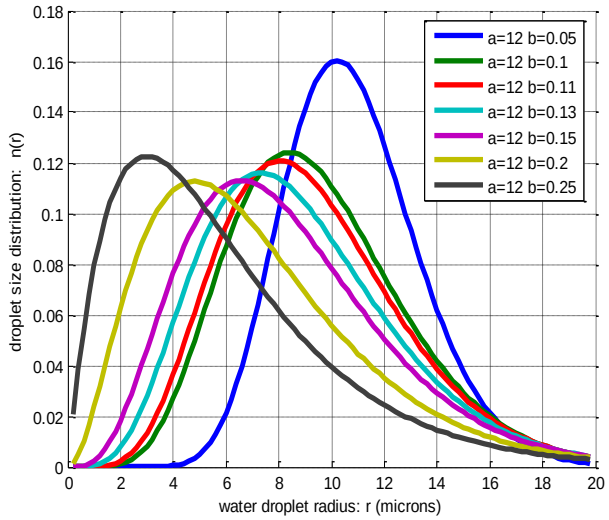

Fig. 2. Gamma DSD with r_e=12 μm and V_e ranging from 0.05 to 0.25.

It should be mentioned that the variability of the DSD is more sensitive to the change of the effective radius than to the changes in the effective variance. The effective radius in Figure 3 ranges from 0 to 40 μm whereas the range of radius in Fig 2 is from 0 to 20 μm. Therefore, controlling the DSD requires monitoring both parameters *a* and *b*.

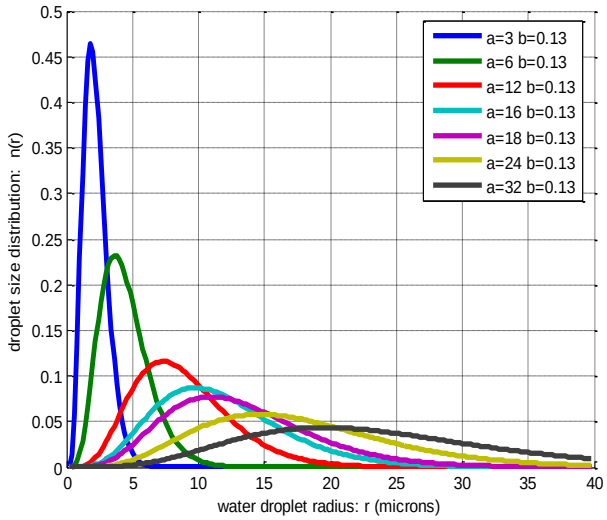

Fig. 3. Gamma DSD with$V_e = 0.13$ and r_e ranging from 3 to 32 μm.

To monitor the evolution of DSD from satellite measurements it is required to extract from data the best estimates for *a* and *b*. The most common values for effective variance in satellite retrieval algorithms are: for the Atmospheric Radiation Measurement (ARM) program assumed DSD with an effective variance value of 0.1 [11]; the International Satellite Cloud Climate Project uses 0.15 [12]; and the Moderate Resolution Imaging Spectrometer (MODIS) team uses 0.13 [8]. Lindsey and Grasso [7] used the following version of the Gamma function:

$$n(D) = AD^{\alpha}e^{-\beta D} \qquad (10)$$

where *D* is the diameter of a droplet, *A* is a constant, and α and β are parameters of the distribution. After replacing *D* with *2r* in eq. (10) and comparing eq. (1) with eq. (10), it can be shown that $\alpha = \frac{1-3b}{b}$. The fact that Lindsey and Grasso (2008) used α=1 implies that they used 0.25 as effective variance.

Figure 4 shows Gamma DSD's using a fixed effective radius at 16 and 50 μm and the most common values of effective variance.

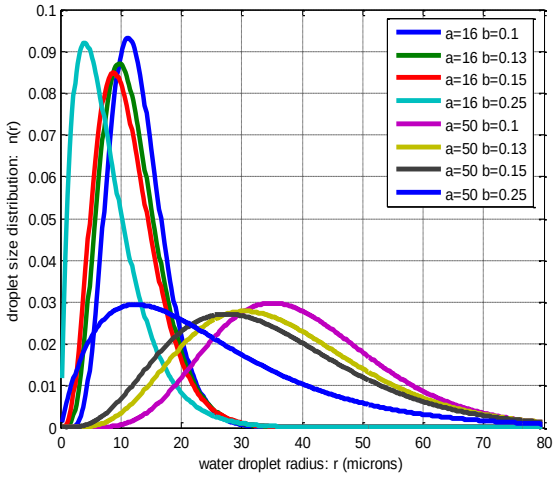

Fig.4. Gamma DSD with common effective variance values used in satellite retrieval algorithms.

3. Monte Carlo simulation and parameter estimation

Monte Carlo simulation techniques were used to generate DSD's. The synthetic data sets were developed with the purpose of recreating the actual DSD for different effective radius and effective variance and also for illustrating the parameter estimation procedure. Figure 5 shows the simulated water DSD for 1000 water droplets with an effective radius of 16 μm and effective variance of 0.13. The maximum likelihood method was also used to estimate the *a* and *b* parameters. It can be shown that the maximum likelihood method provide reliable estimates to the theoretical values. The maximum likelihood estimate for *a* was 16.07 μm and the estimate for *b* was 0.127. Thus, the expected radius and the standard deviation of the radius are 11.98 μm and 4.94 μm, respectively.

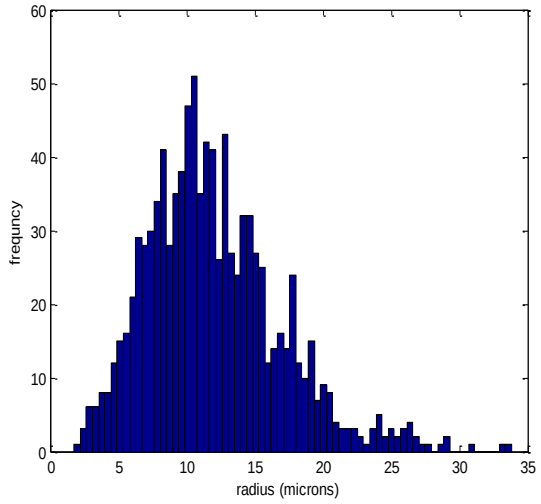

Fig. 5. Simulation of a water DSD for which $a = 16$ μm, and *b*=0.13.

4. Evolution of droplet size distribution from a thick ice cloud

Lindsey and Grasso [7] developed an effective radius retrieval algorithm for thick ice clouds using GOES. This algorithm works properly for clouds with brightness temperature less than 233K. Essentially, this algorithm computes the albedo at 3.9 μm and uses the geometric parameters such as scattering angle and solar zenith angle to estimate the effective radius. Albedo is based on the total radiance of channel 2 (3.9 μm), solar irradiance, and the equivalent black body emitted by thermal radiation at 3.9 μm for a cloud at temperature *T*.

The effective radius retrieval algorithm was used to estimate the evolution of effective radius during a thunderstorm that occurred during May 2005 over the United States [13]. An arbitrary cloud pixel was selected and the effective radius was estimated during approximately three hours. Table 1 shows the location of the pixel, the time and the effective radius. Figure 6 shows the location of the storm and the pixel. Figure 7 shows how the droplet size distribution evolves during the study time interval.

Table 1. Evolution of effective radius

pixel	1	2	3
Latitude	44.77	44.77	43.90
Longitude	-94.26	-94.22	-94.75
UTC time	Effective radius		
11:31	13.08	10.75	28.00
11:45	15.42	12.35	33.51
12:15	29.17	25.04	38.56
12:45	47.90	47.12	50.19
13:01	44.89	45.69	44.96
13:15	41.78	47.04	50.59
13:31	44.35	46.59	38.72
13:45	45.00	43.55	41.15
14:01	48.47	50.16	47.35
14:15	42.76	43.61	39.75
14:31	43.87	42.29	39.94
14:45	43.91	44.10	51.44

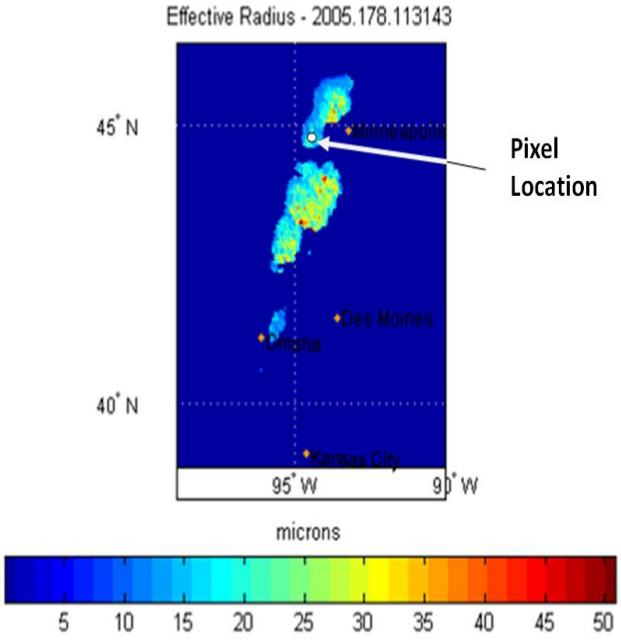

. Figure 6. Effective radius and location of pixel 1.

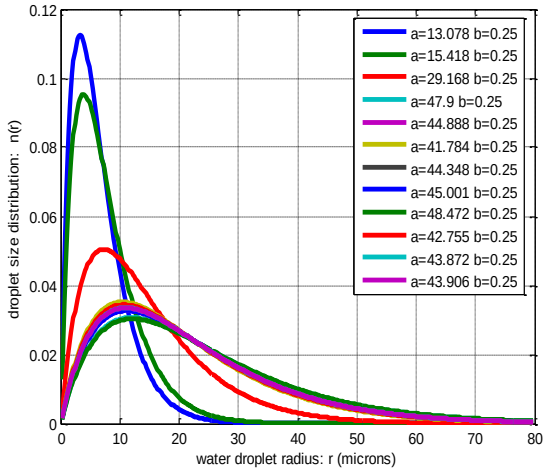

Fig. 7. Evolution of the DSD for pixel 1

5. Detection of warm rainy clouds

Most IR-based satellite rainfall algorithms have been calibrated for very cold convective clouds, and consequently often fail to detect warm rainy clouds, especially over tropical areas, such as Puerto Rico. For example, the Hydro-Estimator [14, 15, 16, 17] was calibrated to estimate rainfall for clouds which have brightness-top temperature below 235K.

It is known that precipitation processes in clouds with warm tops are very sensitive to the microphysical structure of their tops. Specifically, precipitation processes are more efficient when water droplets or/and ice particles grow to larger sizes [18]. It has been shown that the uses of the reflected portion of the near-infrared during the daytime indicates the presence of large cloud-top particles and suggest rain in warm-top clouds. Thus, parameterization of the DSD can be used to detect warm rainy clouds, and the parameterization should estimate both the effective radius and variance. There are algorithms to retrieve effective radius for cold clouds [7]. However, algorithms to retrieve both parameters (effective radius and variance) for warm rainy clouds may not exist. Since substantial research effort is required to develop an appropriate

procedure to retrieve the parameters of the DSD, an indirect measurement of the parameters of the DSD was implemented in this study. The albedo of GOES channel 2 (3.9 μm) was used as a proxy variable of the parameters of the DSD for warm rainy clouds.

Preliminary work is presented here to show that albedo has value for detecting warm rainy clouds. A severe storm that occurred in Puerto Rico on October 27-29, 2007 was selected, with a focus on daytime scenes containing significant numbers of raining pixels with 10.7-μm brightness temperatures above 235K. The study area covers 121x121 radar pixels with a grid size of 0.025^{o} (2.6x2.8km). Rain rate from radar was obtained every 6 or 7 minutes for each pixel. Figure 7 shows the estimates of rain rate based on radar reflectivity.

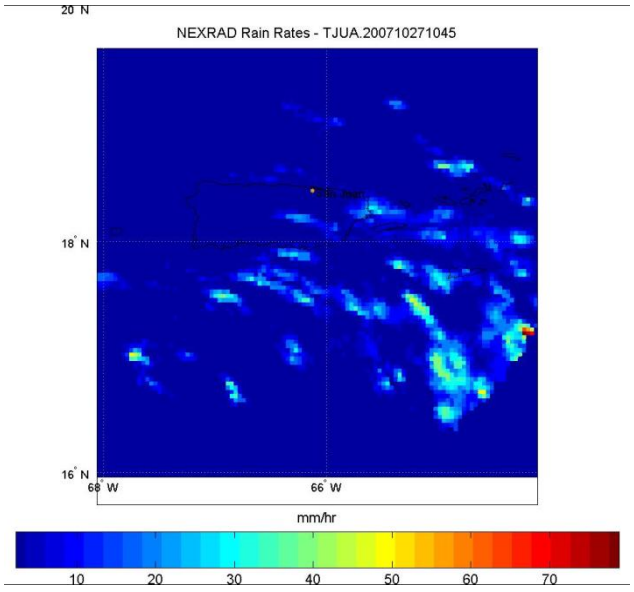

Fig. 7 Rain rate estimated from NEXRAD (Oct. 28, 2007).

GOES data were collected every 15 minutes and comes at approximately $4x4km^2$ spatial resolution. The collected data were organized at every 15 minutes; i.e., radar data were aggregated to match the selected satellite data.

Figure 8 shows the brightness temperature during the same time and space of Figure 7. Figure 9 shows in blue the cold-rain pixels (≤235K) and in red shows the warm-rain pixels (>235K). Pixels with no rain are shown in white. The albedo for the near-infrared channel (3.9-μm) was estimated using the method described in [13]. An artificial neural network (ANN) was trained to differentiate raining (labeled as 1) from nonraining (labeled as 0) pixels for a small sample of data. Two hours of data were used for training and four hours for validation; validation results are presented in Table 2.

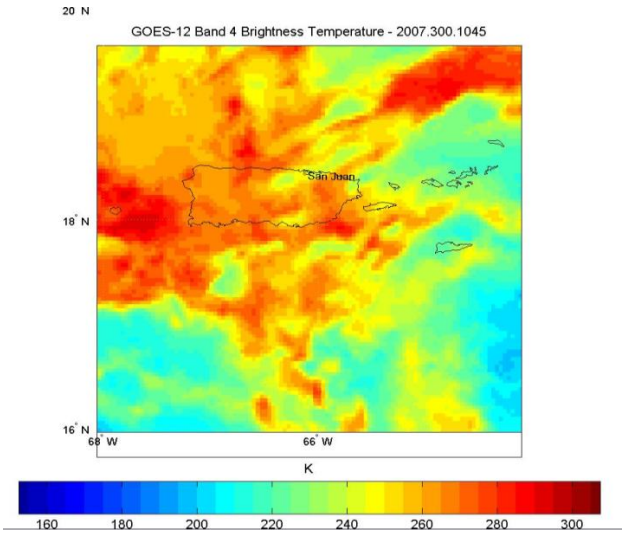

Fig. 8. Brightness temperature for the rainfall event shown in Fig. 7.

Table 2. Validation results for warm rainy cloud event using albedo.

HIT Rate	POD	FAR	BIAS
0.65	0.51	.44	1.70

To improve the warm-rain detection four variables were added to the detection scheme:

- Visible reflectance from channel 1 (0.65 μm)
- Brightness temperature from channel 4 (10.7μm)
- Brightness temperature difference for 3.9μm - 10.7-μm
- Brightness temperature difference for 6.7μm - 10.7μm

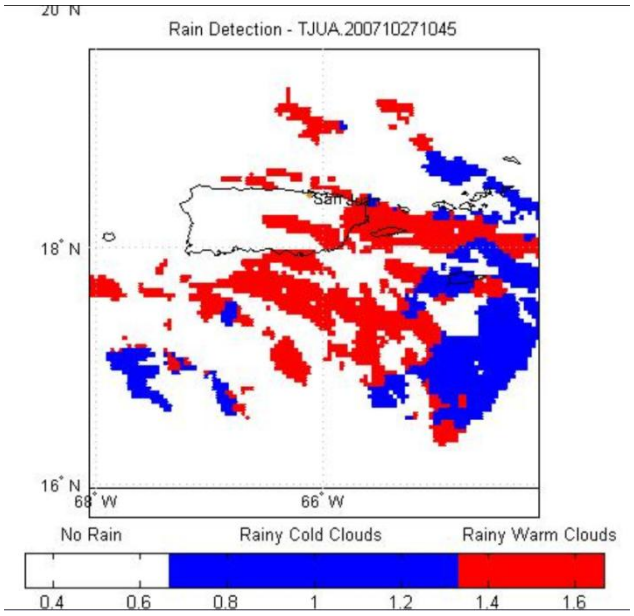

Fig. 9. Rainy pixels from warm and cold clouds.

A variable selection algorithm [19] was used to select the best variables. The selected variables were: albedo, brightness temperature difference (3.9μm – 10.7 μm), and brightness temperature of channel 4 (10.7μm). An ANN was used to detect the rain / no rain pixels and results are shown in Table 3.

Table 3. Validation results for warm rainy cloud event using three variables.

HIT Rate	POD	FAR	BIAS
0.77	0.72	.33	1.08

The 3-variable scheme shows a significant improvement on the validation data over the 1-variable scheme. No comparison was conducted with the Hydro-Estimator (HE) because the HE was not calibrated to work with warm clouds. However, this algorithm can be used to enhance the warm rainy cloud detection of the HE.

6. Conclusions

A statistical analysis of the modified Gamma distribution is presented. It has been shown that the mean and the variance of droplet radius are expressed as functions of both parameters of the distribution, *a* and *b*. However, the effective radius and effective variance are expressed as a single parameter of the distribution *a* and *b*, respectively.

The modified Gamma distribution is the preferred cloud DSD because the major parameter has a physical representation. The effective radius represents the ratio of the typical volume to the projected area.

It is required to estimate two parameters to properly represent the cloud DSD. The evolution of the DSD can be monitored by using effective radius retrieval algorithms. GOES data provides the possibility of monitoring the evolution of thunderstorms because of the rapid refresh (every 15 minutes) over the Continental United States (CONUS) and nearby regions and very short data latency times.

In the absence of an explicit retrieval of these DSD parameters, albedo at 3.9 μm was used as a proxy variable for the parameters and preliminary results show that the explored algorithm is a potential tool to enhance HE detection of rainfall from relatively warm clouds.

7. Acknowledgements.

This research has been supported by NOAA-CREST grant number NA17AE1625, the NSF-ERC-CASA with a grant Number 0313747, NOAA-NWS grant number NA06NWS468001, and also by the University of Puerto Rico at Mayagüez. The authors appreciate and recognize the funding support from these institutions. We want to express our sincere gratitude to Dr. Daniel T. Lindsey for provided us the code to retrieve effective radius of clod clouds.

We also want to appreciate Pieter van der Meer for his contribution in the manuscript editing.

References

[1] Slingo, A. 1990. Sensitivity of the Earth's radiation budget to changes in low clouds. *Nature* 343, 49-51

[2] Kiehl, J. T., and B. P. Briegleb. 1994. A New Parameterization of the Absorptance Due to the 15-μm Band System of Carbon Dioxide**.** *J. Geophys. Res.*, 99:23107-23115.

[3] Dandin, P., C. Pontikis, and E. Hicks (1997), Sensitivity of a GCM to Changes in the Droplet Effective Radius Parameterization, *Geophys. Res. Lett*., 24, 437-440.

[4] Comarazamy D., J.E. González, C.A. Tepley, S. Raizada, and V. Pandya. The effects of atmospheric particle concentration on cloud microphysics over Arecibo, *J. Geophysical. Res*., 111, D09205, DOI:10.1029 /2005JD 0062432006.

[5] Saleeby, M. S., and W. R. Cotton. 2004: A large-droplet mode and prognostic number concentration of cloud droplets in the Colorado State University Regional Atmospheric Modeling System (RAMS) Part I: Module descriptions and supercell test simulations. *J. Applied Meteor*., **43**, 182-195

[6] Hansen, J.E., 1971. Multiple scattering of polarized light in planetary atmospheres, Part II. Sunlight reflected by terrestrial water clouds. *J. Atmospheric Sciences*. **28**, 1400-1426.

[7] Lindsey, D., and Grasso, L., 2008. An effectives radius for thick ice clouds using GOES. *J. Applied Meteor. and Climat.*, **47**, 1222-1231.

[8] Nakajima, T., and M.D. King, 1990. Determination of the Optical Thickness and Effective Particles Radius of Clouds from Reflected Solar Radiation Measurements. Part I: Theory. *J. Atmospheric Sciences*, **47**, 15, 1878-1893.

[9] Arduini, R.F., P. Minnis, W.L. Smith Jr., J.K. Ayers, M.M. Khaiyer, and P. Heck, 2005. Sensitivity of Satellite-Retrieved Cloud Properties to the Effective Variance of Cloud Droplet Size Distribution. *Fifteen ARM Team Meeting Proceedings*, Daytona Beach, FL. 1-13.

[10] Yang, P., K.N. Liou, K. Wyser, and Mitchell, 2000. Parameterization of the scattering and absorption properties of individual ice crystals. *J. Geophys., Res*. 105, 4699-4718

[11] Minnis, P., D.P. Garber, D.F., Arduini, and Y. Takano, 1998. Parameterization of Reflectance and Effective Emittance for Satellite Remote Sensing of Cloud Properties. *J. Atmospheric Sciences*, 55, 3313-3339.

[12] Rossow, W.B. and R.A. Schiffer, 1999. Advances in Understanding Clouds from ISCCP. *Bulletin of the American Meteorological Society*, **80**(10). 2261-2287.

[13] Lindsey, D.T., D. W. Hillger, L. Grasso, J.A. Knaff, and J.F. Dostalek, 2006. GOES Climatyology and Analysis of Thunderstorms with Enhancen 3.9 μm Reflectivity. .*Mon. Wea. Rev*. **134**, 2342-2353.

[14] Scofield, R.A., and R.J. Kuligowski, 2003: Status and outlook of operational satellite precipitation algorithms for extreme-precipitation events. Wea. *Forecasting*, **18**, 1037-1051.

[15]. Harmsen, E. W., S. E. Gomez Mesa, E. Cabassa, N. D. Ramírez-Beltran, S. Cruz Pol, R. J. Kuligowski And R. Vasquez, 2008. Satellite sub-pixel rainfall variability. *International Journal of Systems Applications, Engineering and Development*, No. 3, Vol. 2, pp 91-100.

[16]. Ramírez-Beltran, N.D, Kuligowski, R.J., Harmsen, E., Castro, J.M., Cruz-Pol, S., Cardona-Soto, M. (2008). Rainfall Estimation from Convective Storms Using the Hydro-Estimator and NEXRAD. *WSEAS Transaction on Systems*. No. 10, Vol. 7, pp 1016-1027.

[17] Ramírez-Beltran, N.D, Kuligowski, R.J., Harmsen, E., Castro, J.M., Cruz-Pol, S., Cardona-Soto, M. (2008). Validation and Strategies to Improve the Hydro-Estimator and NEXRAD over Puerto Rico. Proceedings of the 12th *WSEAS International Conference on Systems.* Heraklion, Crete, Greece, July 22-24, pp 799-806.

[18] Lensky, I.M., and D. Rosenfeld, 1997. Estimation of precipitation area and rain intensity based on the microphysical properties retrieved from NOAA AVHRR data. *J. Applied Meteor*., **36**, 234-242.

[19] Ramirez-Beltran, N.D., W.K.M. Lau, A. Winter, J.M. Castro, and N.R. Escalante, 2007: Empirical probability models to predict precipitation levels over Puerto Rico stations. *Mon. Wea. Rev*. **135**, 877-890.

8. Appendix

The k^{th} moment of the distribution is

$$E(r^k) = \int_0^\infty r^k n(r) dr$$

$$= L \int_0^\infty r^{\left(k+\frac{1-3b}{b}\right)} \, e^{-\left(\frac{r}{ab}\right)} dr$$

Let be $u = \frac{r}{ab}$, thus, the above equation can be written as:

$$= L \int_0^\infty (abu)^{\left(k+\frac{1-3b}{b}\right)} \, e^{-\mathrm{u}} \, ab \, du$$

$$= L(ab)^{\left(k-2+\frac{1}{b}\right)} \int_0^\infty (u)^{\left(k-3+\frac{1}{b}\right)} e^{-\mathrm{u}} \, du$$

$$= L(ab)^{\left(k-2+\frac{1}{b}\right)} \Gamma\left(k-2+\frac{1}{b}\right) \qquad A(1)$$

The expected value of the radius is obtained after replacing k by 1 in the previous equation.

$$E(r) = L(ab)^{\left(\frac{1}{b}-1\right)} \Gamma\left(\frac{1}{b}-1\right) = \frac{ab\,\Gamma\left(\frac{1}{b}-1\right)}{\Gamma\left(\frac{1}{b}-2\right)} \qquad (A2)$$

Knowing that $\Gamma(s+1) = s\Gamma(s),\ s > 0$ eq. (*A2*) can be written as:

$$E(r) = \frac{ab\,\left(\frac{1}{b}-2\right)\Gamma\left(\frac{1}{b}-2\right)}{\Gamma\left(\frac{1}{b}-2\right)} = a(1-2b)$$

The variance of the radius can be computed as follows:

$$V(r) = \int_0^\infty \left(r - E(r)\right)^2 n(r) dr$$

$$= E(r - E(r))^2 = E(r^2) - [E(r)]^2$$

$$= L\,ab\,(ab)^{\left(\frac{1}{b}\right)} \Gamma\left(\frac{1}{b}\right) - \, a^2(1-2b)^2$$

$$= \frac{(ab)^2 \Gamma\left(\frac{1}{b}\right)}{\Gamma\left(\frac{1}{b}-2\right)} - a^2(1-2b)^2 \qquad (A3)$$

Consider

$$\frac{\Gamma\left(\frac{1}{b}\right)}{\Gamma\left(\frac{1}{b}-2\right)} \qquad (A4)$$

Using the following identity: $\Gamma(s) = \frac{1}{s}\Gamma(s+1)$, thus if $s = \frac{1}{b} - 2$, $\Gamma\left(\frac{1}{b}-2\right) = \frac{\Gamma\left(\frac{1}{b}-1\right)}{\left(\frac{1}{b}-2\right)}$, Therefore, eq.(A4) can be written as follows:

$$\frac{\Gamma\left(\frac{1}{b}\right)}{\Gamma\left(\frac{1}{b}-2\right)} = \frac{\Gamma\left(\frac{1}{b}\right)\left(\frac{1}{b}-2\right)}{\Gamma\left(\frac{1}{b}-1\right)} = \frac{\Gamma\left(\frac{1}{b}\right)\left(\frac{1}{b}-2\right)\left(\frac{1}{b}-1\right)}{\Gamma\left(\frac{1}{b}\right)}$$

$$= \frac{1}{b^2}(1 - 3b + 2b^2) \qquad (A5)$$

Therefore, replacing (A5) into (A3) the variance of the radius can be expressed as:

$$V(r) = a^2 b^2 \frac{1}{b^2}(1 - 3b + 2b^2) - a^2(1-2b)^2$$

$$= a^2 b(1-2b) \qquad (A6)$$

The effective radius can be computed as follows:

$$\frac{E(r^3)}{E(r^2)} = \frac{L(ab)^{\left(1+\frac{1}{b}\right)}\Gamma\left(1+\frac{1}{b}\right)}{L(ab)^{\left(\frac{1}{b}\right)}\Gamma\left(\frac{1}{b}\right)} = ab\frac{\Gamma\left(1+\frac{1}{b}\right)}{\Gamma\left(\frac{1}{b}\right)} \qquad (A7)$$

Using $\Gamma(s) = \frac{1}{s}\Gamma(s+1)$, and $s = \frac{1}{b}$, it follows that

$$\Gamma\left(\frac{1}{b}+1\right) = \frac{1}{b}\Gamma\left(\frac{1}{b}\right)$$

Therefore, (A7) can be written as follows:

$$\frac{E(r^3)}{E(r^2)} = ab\frac{\frac{1}{b}\Gamma\left(\frac{1}{b}\right)}{\Gamma\left(\frac{1}{b}\right)} = a \qquad (A8)$$

The effective variance is defined as follows:

$$V_e = \frac{\int_0^\infty (r-a)^2 r^2 n(r) dr}{a^2 \int_0^\infty r^2 n(r) dr} \qquad (A9)$$

Consider only the numerator of (A9)

$$\int_0^\infty (r-a)^2 r^2 n(r) dr$$

$$= \int_0^\infty (r^4 - 2r^3 a + r^2 a^2) n(r) dr$$

$$= E(r^4) - 2aE(r^3) + a^2 E(r^2)$$

$$= L(ab)^{\left(2+\frac{1}{b}\right)}\Gamma\left(2+\frac{1}{b}\right) - 2aL(ab)^{\left(1+\frac{1}{b}\right)}\Gamma\left(1+\frac{1}{b}\right)$$

$$+ a^2 L(ab)^{\left(\frac{1}{b}\right)}\Gamma\left(\frac{1}{b}\right) \qquad (A10)$$

Replacing (A10) into (A9) the effective variance can be written as follows:

$$\frac{L(ab)^{\left(2+\frac{1}{b}\right)}\Gamma\left(2+\frac{1}{b}\right) - 2aL(ab)^{\left(1+\frac{1}{b}\right)}\Gamma\left(1+\frac{1}{b}\right) + a^2 L(ab)^{\left(\frac{1}{b}\right)}\Gamma\left(\frac{1}{b}\right)}{a^2 L(ab)^{\left(\frac{1}{b}\right)}\Gamma\left(\frac{1}{b}\right)}$$

$$= \frac{b^2\Gamma\left(2+\frac{1}{b}\right) - 2b\Gamma\left(1+\frac{1}{b}\right) + \Gamma\left(\frac{1}{b}\right)}{\Gamma\left(\frac{1}{b}\right)}$$

$$= \frac{b\left(1+\frac{1}{b}\right)\Gamma\left(\frac{1}{b}\right) - 2\Gamma\left(\frac{1}{b}\right) + \Gamma\left(\frac{1}{b}\right)}{\Gamma\left(\frac{1}{b}\right)} = b$$